Isotope Study on Diffusion in $CaSO_4$ Formed During Sorbent-Flue-Gas Reaction

C. Hsia and G. R. St. Pierre
Dept. of Materials Science and Engineering

L.-S. Fan
Dept. of Chemical Engineering
Ohio State University, Columbus, OH 43210

In sorbent-flue-gas reactions, porous CaO sorbent particles are used to capture SO_2 by formation of $CaSO_4$. The overall reaction can be expressed by reaction 1:

$$CaO_{(S)} + SO_{2(g)} + \frac{1}{2}O_{2(g)} = CaSO_{4(S)} \qquad (1)$$

Because of the large molar volume of $CaSO_4$, the internal surface area which is originally available for reaction diminishes as $CaSO_4$ forms. Formation of $CaSO_4$ on CaO has a twofold effect. First, $CaSO_4$ covers the fresh CaO surface and blocks the passage between CaO and the gas. Secondly, volumetric expansion upon conversion results in plugging of the pores in the CaO. Subsequently, the passages between the sorbent and the flue gas are blocked. For these reasons, CaO sorbents become "deactivated" and the rate of sorbent sulfation decreases. Once the $CaSO_4$ layer forms, further sorbent sulfation is believed to be controlled by the product layer diffusion process (Borgwardt et al., 1987). It has been suggested that the product layer diffusion occurs by gaseous diffusion (Simons and Garman, 1976) and by ionic diffusion (Bhatia and Perlmutter, 1981).

In examining ionic diffusion mechanisms through the $CaSO_4$ product layer by marker experiments, Hsia et al. (1993) found that the inert platinum markers were embedded between CaO and $CaSO_4$. They concluded that the product layer thickens by the outward growth mode in which Ca^{2+} and O^{2-} ions diffuse in a coupled manner from the inner $CaO/CaSO_4$ interface to the outer $CaSO_4$/gas interface. At the $CaSO_4$/gas interface, the sulfation reaction takes place as follows:

$$Ca^{2+} + O^{2-} + \frac{1}{2}O_2 + SO_2 = CaSO_4 \qquad (2)$$

From crystal structure considerations, they further suggested that it is unlikely to have significant SO_4^{2-} ion diffusion through the $CaSO_4$ layer.

In the inert marker experiment, because of not participating in the reaction, the markers should always reside on the interface where the ions with higher diffusivity are generated. Therefore the opposite interface, where the slower ions are formed, should become the sulfation site. On the other hand, the present work uses a "two-stage" sulfation technique to determine the growth mode of $CaSO_4$. As to be explained later, the location enriched with isotope ^{34}S will be the site for sulfation reaction described in Eq. 1. In fact, ^{34}S can be viewed as a "reactive" marker which will reside on the sulfation site. Nevertheless, it is not called this way to avoid confusion with the inert marker technique. These two experiments are to be regarded complementary in the sense that, for the same reaction, location of the inert and the reactive markers should always be on the opposite sides of the product layer. Based on this understanding, results obtained from the present sulfation experiments can be correlated with the previous work (Hsia et al., 1993) and, additionally, compared with ionic diffusion in crystals of similar structure.

Experimental Studies

The "two-stage" reaction technique is often used in studies of gas-solid reactions, such as in metal oxidation (Atkinson and Smart, 1988; Moon, 1990) and metal sulfidation (Gilewicz-Wolter, 1990). Initially, in a two-stage reaction, the solid is reacted with the first gaseous oxidant at a fixed temperature for a given period of time. After the first period of reaction is terminated, the second gaseous oxidant, an isotope of the first oxidant, replaces the first oxidant and reacts for another period of time. At the end of the two-stage reaction, the solid is generally analyzed in a secondary ion mass spectrometer (SIMS). If the reaction is controlled by solid state diffusion, the growth mode of the product layer can be identified by the relative concentrations of oxidants in the product.

Correspondence concerning this article should be addressed to G. R. St. Pierre or L.-S. Fan.
Current address of C. Hsia: U.S. Steel, Research, Monroeville, PA 15146.

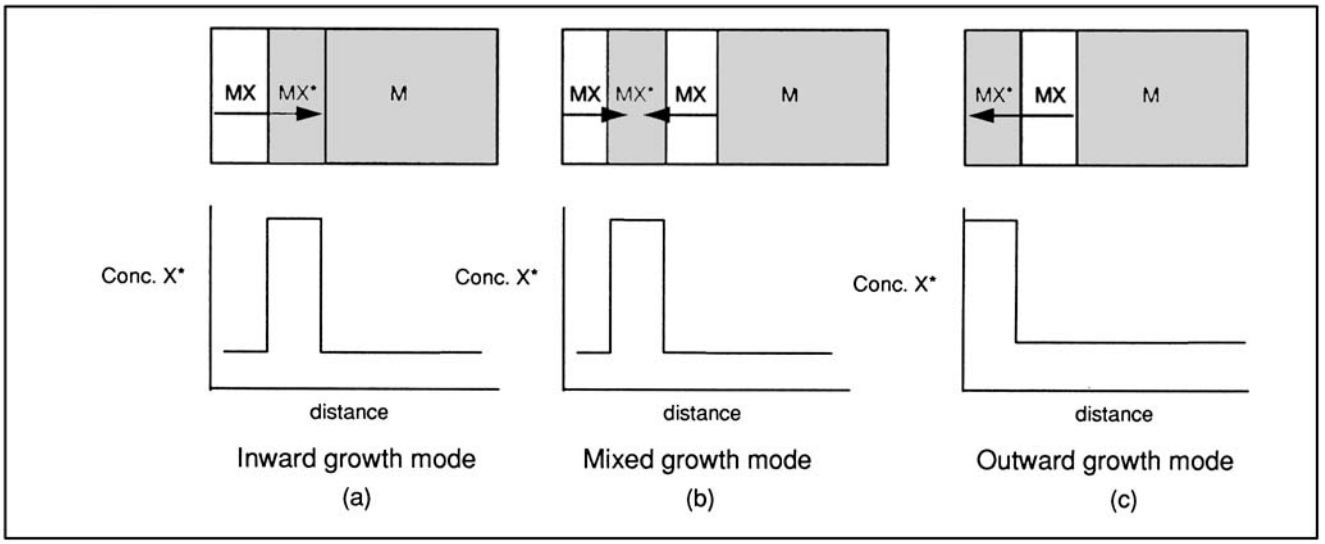

Figure 1. Concentration profiles.

(a) Inward growth mode; the MX* layer is found next to the solid/solid interface; (b) mixed growth mode; one additional interface is present, the MX* layer is sandwiched between two MX layers; (c) outward growth mode; the MX* layer is found next to the gas/solid interface.

In the SIMS analysis, the specimen surface is bombarded with an ion beam of high speed. Upon bombardment (or sputtering), the elements on the specimen are ionized and are directed toward a mass spectrometer. Normally, if the sputtering rate (μm/s) is known, by measuring the sputtering time, the concentration profile of the specimen can be obtained. Suppose that, in the two-stage reaction, oxidant X is used first and followed by its isotope X*. When the solid is denoted by M and the reaction product by MX, the concentration profiles of X* in the inward, mixed and outward growth modes should resemble those shown in Figure 1.

In Figure 1, arrows are used to indicate the directions of ionic transport. The origin of an arrow represents the supply of ionic species while the arrowhead points to, in the present study, the sulfation site. Figure 1a shows the inward growth mode in which the ion generated at the gas/solid interface has a higher mobility than that generated at the solid/solid interface; the new product layer MX* thus forms at the solid/solid interface. In Figure 1c, the reverse is true because the ion formed at the solid/solid interface has a higher mobility than that formed at the gas/solid interface; therefore, an outward growth mode is observed. In Figure 1b, assuming comparable rates of the two modes, the MX* layer is shown to form between two layers of MX. The relative thicknesses of the two MX layers will depend on the relative rates of two competing ionic diffusion modes. Figures 1a and 1c represent the two limiting cases while Figure 1b is the general case. Schematic concentration profiles of X* in these three cases are also drawn corresponding to the growth modes. Therefore, by sputtering the specimen surface and obtaining the concentration profile, the growth mode of the product layer can be identified.

In this work, a two-stage sulfation experiment using $^{32}SO_2$ and $^{34}SO_2$ was performed. Pure CaO powder (Aldrich chem., 99.95%) was pressed into tablets and subsequently sintered in air at 1,400°C for 24 h. The sintered CaO tablets appearing white in color were placed on a platinum foil. The foil was then placed on an Al_2O_3 boat and pushed into the mullite tube. Figure 2 shows the experimental setup in the present work.

For the first stage of sulfation, at 1,300°C, 5,000 ppm $^{32}SO_2$/air mixture was passed into the mullite tube and circulated out through the bubbler continuously. This stage lasted for 14 days. When the first stage was terminated, the tablets were removed from the furnace and examined. The tablets appeared slightly yellowish, which is believed to be due to the $CaSO_4$ formation. Tablets were then again placed on the platinum foil and pushed into the mullite tube for the second stage sulfation. At the beginning of the second stage sulfation, 5,000 ppm $^{32}SO_2$/air mixture was first used during the heating period. As soon as the tube temperature reached 1,300°C, the mechanical pump was turned on and the pressure in the tube was reduced immediately. The required pumping time was within 20 s since the experimental system was relatively small. Upon the completion of the evacuation, isotope gas 75%$^{34}SO_2$-25%$^{32}SO_2$ was introduced into the mullite tube. Appropriate amount of air was also introduced into the tube such that the total SO_2 concentration was roughly 5,000 ppm. The second stage sulfation lasted for three days. The SIMS analysis was performed by Microelectronics Center in North Carolina.

Results and Discussion

Profilometry traces were performed on a specimen before the SIMS analysis. Figures 3 and 4 show that the specimen surfaces were very rough. The highest and the lowest points on the surface differ by as much as 50 μm. Because of this surface roughness, even with a well-known sputtering rate, estimation of the concentration profiles in the specimens was difficult. Therefore, the concentration profile cannot be extracted quantitatively from the present result. The relative

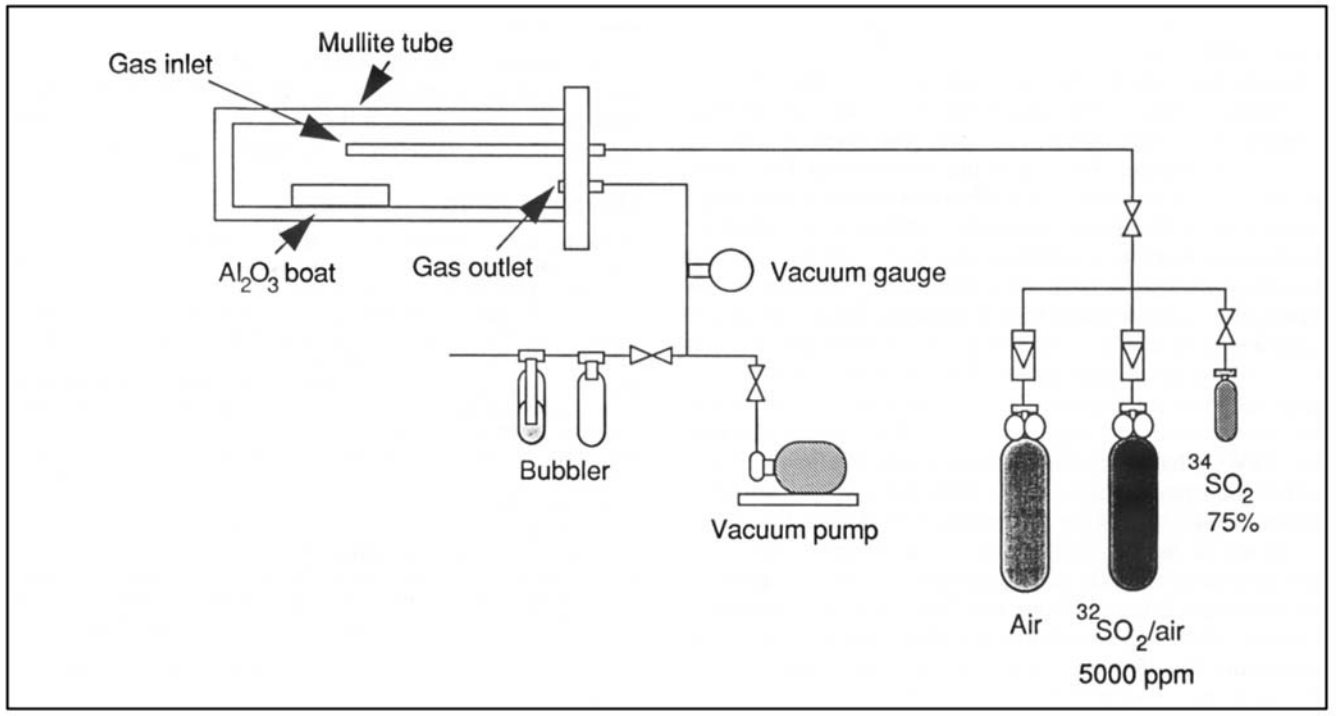

Figure 2. Experimental setup.

concentration (counts/s) as a function of depth (sputter time), however, does yield the necessary qualitative information to determine the growth mode of $CaSO_4$.

The SIMS analyses, as given in Figure 5, show that the intensity of ^{34}S is the highest at the outer specimen surface. From sputter time 0 min to approximately 5.5 min, the ^{34}S intensity decreases continuously. After 5.5 min, the intensity remains relatively flat up to 113.5 min. Since the ^{34}S intensity at the surface is more than one order of magnitude higher than that in the remaining portion of the specimen, there is definitely an enrichment of ^{34}S at the surface. Generally, the ratio between ^{32}S and ^{34}S in naturally occurred sulfur is 22.6. In the present analysis, if 1/22.6 is taken as the $^{34}S/^{32}S$ ratio for the flat portion, the $^{34}S/^{32}S$ ratio at the surface is greater than 1/2.26. Consequently, the enrichment of ^{34}S at the surface, as compared to Figure 1c, indicates that $CaSO_4$ thickens following the outward growth mode. The present work agrees with the previous work (Hsia et al., 1993) that when

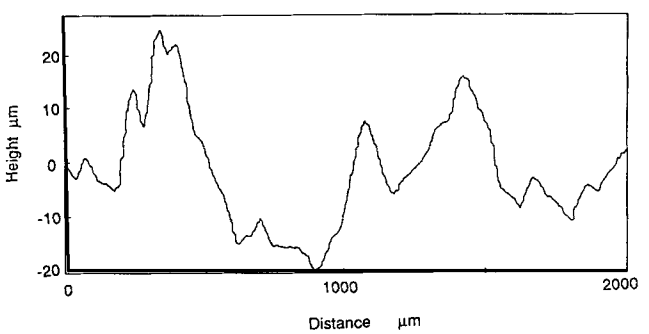

Figure 3. Profilometry trace of the sulfated specimen with very rough specimen surface.

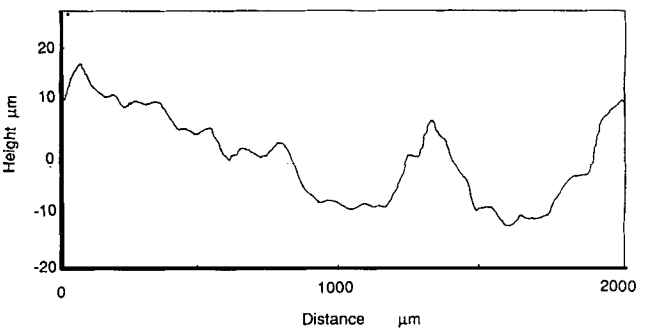

Figure 4. Profilometry trace of the sulfated specimen with a very rough surface.

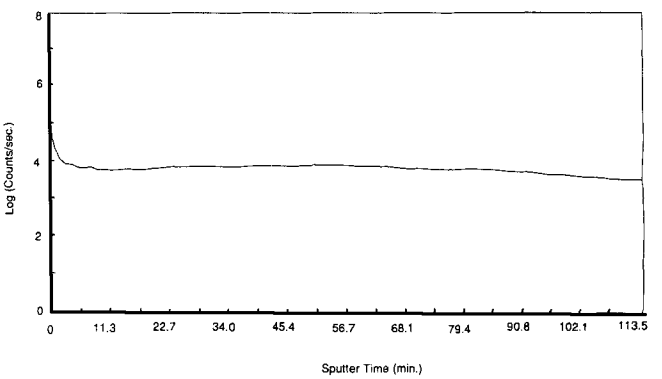

Figure 5. SIMS analysis on ^{34}S as a function of sputter time.

The intensity of ^{34}S appears the highest at the specimen surface, decreases continuously and remains unchanged after about 5.5 min. of sputtering.

controlled by solid state diffusion, $CaSO_4$ grows by the outward growth mode.

$CaSO_4$ has a rhombohedral structure with a distorted zircon lattice ($ZrSiO_4$) (Wyckoff, 1960). Ca^{2+} ions are located between SO_4^{2-} ions which are more than twice as large as the Ca^{2+} ions in size. Because of the arrangement, Ca^{2+} ions should be able to move in the channels between the SO_4^{2-} ions as long as the electroneutrality condition is preserved. In the previous work, it is proposed that Ca^{2+} and O^{2-} diffuse in a coupled manner from the $CaO/CaSO_4$ interface to the $CaSO_4$/gas interface when $CaSO_4$ thickens. Since cations are generally more mobile, a review on the mobility of O^{2-} ion in zircon lattices is appropriate. Lu and Steele (1986) measured the ionic conductivity of CaO doped $BiVO_4$, which has the zircon lattice, and suggested $V_o^{\cdot\cdot}$ is the main charge carrier. $CaWO_4$ has a scheelite structure which is another version of the zircon lattice, that is, more compact and complex (Evans, 1964). Nassau and Loiacono (1963) used the words "....a sea of mobile oxygen ions...." to describe the transport process in $CaWO_4$ and suggested V''_{Ca} and $V_o^{\cdot\cdot}$ pairs as the dominant defects. Gupta and Weirick (1967) measured the tracer diffusivity of calcium in $CaWO_4$ and drew a similar conclusion. On the other hand, Rigdon and Grace (1973) proposed the anti-Frenkel pairs $V_o^{\cdot\cdot}$ and O_i'' which are the dominant defects. Two other crystals, $PbMoO_4$ and $PbWO_4$, also have the scheelite structure. van Loo (1975) proposed that in both of these crystals Schottcky pairs of V''_{Pb} and $V_o^{\cdot\cdot}$ are the predominant defects. In contrast, Groenink and Binsma (1979) measured the electrical conductivity of $PbMoO_4$ and $PbWO_4$ and suggested $V_o^{\cdot\cdot}$ and O_i'' are responsible for the ionic conduction. Arora et al. (1983) proposed $V_o^{\cdot\cdot}$ and O_i'' are the mobile defects in $Ca(WO_4)_x(MoO_4)_{1-x}$.

Despite these differences in the proposed defect structures in the scheelite lattices, all of the above work agrees on the high mobility of oxygen ions. Similar characteristics ought to be found in $CaSO_4$, since it has a less compact structure that allows O^{2-} ions to move more freely. High mobility of O^{2-} ions should not be surprising since the corners of an SO_4^{2-} tetrahedron are connected to corners of other SO_4^{2-} tetrahedra and the nearest neighbor jumps of the oxygen ions should be favored. Therefore, the path formed by the interconnected oxygen sites and the channels formed by the SO_4^{2-} ions make it possible for O^{2-} and Ca^{2+} to move in a coupled manner in CaO_4.

Conclusion

The present two-stage reaction study with $^{34}SO_2$ supports earlier work in establishing that the growth of the $CaSO_4$ occurs primarily by coupled diffusion of Ca^{2+} and O^{2-} from the $CaO/CaSO_4$ interface to the $CaSO_4$/gas interface.

Literature Cited

Arora, K., R. S. Godbole, and D. Lakshminarayana, "Lattice Disorder and Electrical Conductivity of Flux-Grown $Ca(WO_4)_x(MoO_4)_{1-x}$," *J. of Mater. Sci.*, **18**, 1359 (1983).

Atkinson, A., and D. W. Smart, "Transport of Nickel and Oxygen during the Oxidation of Nickel and Dilute Nickel/Chromium Alloy," *J. Electrochem. Soc.*, **135**, 2886 (1988).

Bhatia, S. K., and D. D. Perlmutter, "The Effect of Pore Structure on Fluid-Solid Reactions: Application to the SO_2-Lime Reaction," *AIChE J.*, **27**(2), 226 (1981).

Borgwardt, R. H., K. R. Bruce, and J. Blake, "An Investigation of Product Layer Diffusivity for CaO Sulfation," *Ind. Eng. Chem. Res.*, **26**, 1993 (1987).

Evans, R. C., *An Introduction to Crystal Chemistry*, 2nd ed., Cambridge Univ. Press, Cambridge (1964).

Gilewicz-Wolter, J., "The Use of ^{18}O and ^{35}S Isotopes in Studying the Mechanism of Matter Transport in Scaled Formed on Iron and Cobalt in SO_2 Atmospheres," *Pol. Acad. of Sci. Chem.*, **33**, 53 (1985).

Groenink, J. A., and H. Binsma, "Electrical Conductivity and Defect Chemistry of $PbMoO_4$ and $PbWO_4$," *J. Solid State Chem.*, **29**, 227 (1979).

Gupta, Y. P., and L. J. Weirick, "Diffusion of Calcium in Calcium Tungstate Single Crystals," *J. Phys. Chem. Solids*, **28**, 2545 (1967).

Hsia, C., G. R. St. Pierre, K. Raghunathan, and L.-S. Fan, "Diffusion through $CaSO_4$ formed during the Reaction of CaO with SO_2 and O_2," *AIChE J.*, **39**(4), 698 (1993).

Lu, T., and B. C. H. Steele, "Electrical Conductivity of Polycrystalline $BiVO_4$ Samples Having the Scheelite Structure," *Solid State Ionics*, **21**, 889 (1986).

Moon, D. P., "Duplex Scale Formation During High-Temperature Oxidation of Ni-0.1 wt.% Al Alloy," *Oxidation of Metals*, **31**, 71 (1990).

Nassau, K., and G. M. Loiacono, "Calcium Tungstate-III Trivalent Rare Earth Substitution," *J. Phys. Chem. Solids*, **24**, 1503 (1963).

Rigdon, M. A., and R. E. Grace, "Electrical Charge Transport in Single Crystal $CaWO_4$," *J. Am. Cerm. Soc.*, **56**, 475 (1973).

Simons, G. A., and A. R. Garman, "Small Pore Closure and the Deactivation of the Limestone Sulfation Reaction," *AIChE J.*, **32**(9) (1976).

van Loo, W., "Crystal Growth and Electrical Conduction of $PbMoO_4$ and $PbWO_4$," *J. Solid State Chem.*, **14**, 359 (1975).

Wyckoff, R. W. G., *Crystal Structures*, 2nd ed., Vol. 3, Interscience Pub., New York (1960).

Manuscript received June 13, 1994, and revision received Nov. 7, 1994.